# APPLICATION OF MESOPOROUS SILICA MATERIALS FOR THE IMMOBILIZATION OF POLYPHENOL OXIDASE

Paula Corell Escuin[a], Alfonso García-Bennett[b], Jose Vicente Ros-Lis[a], Angel Argüelles Foix[a], Ana Andrés[a*]

[a] *Instituto de Ingeniería de Alimentos para el Desarrollo. Universitat Politècnica de Valencia. Camino de Vera s/n. Valencia (Spain).*

[b] *Department of Material and Environmental Chemistry (MMK), Stockholm University (SU) SE-106 91 Stockholm, Sweden.*

**Corresponding author. Tel: +34 963877365. Email: aandres@upv.es*

## ABSTRACT

The ability of a number of mesoporous silica materials (SBA-15, SBA-3, and MCM-48) to immobilize polyphenol oxidase (PPO) at different pH has been tested. Pore size and volume are the structural characteristics with higher influence on the PPO immobilization. Mesoropous material SBA-15 adsorbs a larger quantity of PPO at pH 4.00 and offers an inhibition of enzymatic activity close the 50% in apple extracts.

Keywords: polyphenol oxidase; silica materials; inhibition; thiol functionalization

## 1. INTRODUCTION

The control of enzymatic browning is of great economic importance in processed fruits and vegetables. It affects negatively the attributes of colour, taste, flavour and nutritional value of

fruits and vegetables. It is estimated that more than 50% of the fruit market losses are a result of enzymatic browning (Whitaker & Lee, 1995).

Several methods have been proven for the inhibition of PPO activity. Sulphites are used as agents to prevent browning, but are also associated with severe allergies in certain vulnerable populations, limiting their presence in food or beverages (Sapers & Miller, 1993). Heat treatments are unsuitable to inhibit such reactions, due to the detriment in nutrient and vitamin content and they can even increase browning reactions (Toribio & Lozano, 1986). Whereas addition of ascorbic acid (Denoya, Ardanaz, Sancho, Benítez, González & Guidi, 2012; Gacche, Zore & Ghole, 2003), anoxic conditions (Rocha & Morais, 2001), refrigeration and non-thermic treatments (Perez-Gago, Serra & Del Rio, 2006; Olivas, Mattinson & Barbosa-Cánovas, 2007) have shown good results, their industrial application is not widely developed due to the economic cost or the induction of variations in the organoleptic properties.

Thus, there is a necessity for new methods to inhibit PPO activity in fruits and vegetables. To this effect nanomaterials, in particular high surface area silica based mesoporous materials exhibit properties suitable for irreversible enzyme binding and inhibition. Additionally, they show no apparent toxicity (Fu, Liu, Li, Liu, Chen, & Tang, 2013), their structure includes space for functional groups and a high density of silanol groups able to offer pH dependent electrostatic interactions. This feature provides numerous possibilities for selecting these materials as carriers, adsorbents and supports, or for further reactions with organic functional groups. Consequently, their application has been explored within the food sector in various fields such as catalysis, synthesis of nutritional compounds, as sensors or in the controlled release of bioactive molecules (Bernardos & Kourimska, 2013). However, few studies have focused on the mesoporous material–enzyme interaction with relevance to the food industry (Arroyo, 1998; Datta, Christena & Rajaram, 2013; Kupferschmidt, Csikasz, Ballell, Bengtsson & Garcia-Bennett, 2014). Encapsulation of PPO to

47 detect phenolic compounds (Mangrulkar, Yadav, Meshram, Labhsetwar & Rayalu, 2012) or to
48 produce *o*-diphenols in vitro has been demonstrated (Marín-Zamora, Rojas-Melgarejo, García-
49 Cánovas & García-Ruiz, 2009), but the inhibitory activity of such materials with respect to PPO
50 activity was not explored. In this context, the aim of the present article is to perform a prospective
51 study of the potential of various silica mesoporous materials as immobilizing or sequestering
52 agents for polyphenol oxidases from fruits or vegetables.
53
54 **2. MATERIALS AND METHODS**
55 **2.1 Characterization of mesoporous materials**
56 Mesoporous materials SBA-15, SBA-3 and MCM-48 were selected due to their different
57 morphological and textural characteristics. The three materials were prepared according to
58 already well known procedures (Zhao et al., 1998; Anunziata, Beltramore, Martinez & Bellon,
59 2007; Wang, Wu, Sun & Zhong, 2001) and nitrogen adsorption studies, scanning and transmission
60 electron microscopy (SEM, TEM) were performed. The degree of microporosity was calculated
61 from a t-plot analysis and the pore size calculated from Density Functional Theory (DFT). See
62 electronic supporting information for further details.
63 **2.2 PPO enzyme-silanol surface interation**
64 In order to study the PPO enzyme-silanol surface interaction and aiming to explore a future
65 industrial use of this kind of materials as inhibitors, available commercial PPO was used (PPO
66 lyophilized powder from mushroom, 3130 units·mg$^{-1}$ from Sigma-Aldrich). Short contact times
67 (from 15 minutes) and different pH (pH 1, 3, 4, 5 and 7) were tested. The Bradford method
68 (Bradford, 1976) was used to determine the amount of enzyme.

Sampling times were stablished at 0, 15, 30, 60, 120, 360 and 1.440 min in order to follow the kinetics of the immobilization process. The measurement was done five independent times for each mesoporous materials tested.

The immobilization process was modelled by the application of the Power Law (Wise, 1985) and Higuchi equations (Higuchi, 1961). These are standard models to describe the drug release kinetics from a solid porous matrix based on diffusion and derived from by Fick's laws. Here they have been used to explain the kinetics of enzyme adsorption (the opposite to drug release) within the mesoporous matrices. Both Power law and Higuchi model assume that the drug diffuses from inside the porous matrix outwards and as the drug is released, the distance the remaining drug has to travel increases. The amount of drug released is proportional to the square root of time in the case of the Higuchi equation (Higuchi, 1961).

The DFT calculations were developed using the Micromeritics software package TriStar 2030 (Micromeritics Instruments Corp., Atlanta, USA) which provides a method to fit nitrogen isotherms curves from mean-field density functional theory to determine pore size distribution assuming a cylindrical or cage type pore geometries (see i.e. Olivier, Conklin & Szombathely, 1994)

Additionally, extracts of PPO were obtained from apples and were used to test and confirm the material performance observed in the commercial one. PPO extracts were obtained from Granny Smith cultivar apples according to the method proposed by Guerrero (2009). Then, 15 mg of SBA-15 were added in the presence of 5 mL of extract diluted to 15 mL with phosphate buffer at pH 4. The variation in the activity was monitored at diverse times after contact with the material during one hour.

## 3. RESULTS AND DISCUSSION

The three materials are composed of silica and include porous systems with diverse sizes and topology, i.e. while SBA-15 and SBA-3 show 2D hexagonal pore structures with larger and smaller

93 pores respectively, MCM-48 offers a 3D connected cylindrical system of pores. Nitrogen
94 adsorption studies, scanning and transmission electron microscopy (SEM, TEM) confirmed the
95 textural and morphological characteristics of the materials (see table 1) (Zhao et al., 1998;
96 Anunziata, Beltramore, Martinez & Bellon, 2007; Wang, Wu, Sun & Zhong, 2001).
97 According to the pore size, SBA-15 possesses the largest pore size (133 Å), SBA-3 shows the
98 smallest pore size (29.2 Å) and MCM-48 is lying in between with a pore size of 33.4 Å (Table 1).
99 The only material which has micropores is SBA-15 with two different pore sizes in the microporous
100 range (10.6 Å and 20.0 Å), in addition to its mesoporosity.
101 A summary of the amount of enzyme immobilized by each material at diverse times and pH can
102 be found in Figure 1. The standard deviation was never higher than 0.03. For clarity purposes a
103 graph plotting the amount of PPO adsorbed by the different materials at different pH values after
104 1 hour of contact time has been included as Figure 2.
105 A general view of the figure 1 graphs shows that, in general, the immobilization of the enzyme is
106 not a fast process and increasing the material-enzyme interaction time increases the amount of
107 PPO immobilized on the silica walls. The data also reveals that the immobilization rate is strongly
108 dependent on both, material textural properties as well as pH. On the contrary, the channel
109 configuration (2D-hexagonal channels for SBA-15 and SBA-3, a 3D-channel structure for MCM-48)
110 is not of particular relevance.
111 SBA-15 at pH 4 offers the highest and fastest loading capacity, being able to load an equivalent
112 amount of enzyme higher than 30 % of its mass even at very short times (the first sampling point
113 was stablished at 15 minutes). Similar results are obtained at pH 3. In contrast, SBA-3 and MCM-
114 48 show slower processes in particular at pH 1 or 7. Since all the materials are composed of silica,
115 a similar behaviour can be expected as a response to pH variations; in fact, Figure 2 shows that pH
116 4 offers the maximum capacity of immobilization of PPO for all the materials, followed closely by

pH 3; in contrast, the pH value which shows the minimum quantity of enzyme immobilized was in all cases pH 7.

Knowing the structural and morphological properties of the tested materials allows understanding the results of the immobilization assays. Materials having higher pore volume and bigger pore size (SBA-15) can immobilize more PPO than those with low pore volume and size (MCM-48) and the process is faster. Taking into account the similarity of pore volume between the SBA-15 and the SBA-3, the pore size seems to be the key parameter. As the pore size increases, PPO can diffuse more easily and is free to interact with the silanol groups of the silica walls than in materials such as SBA-3 or MCM-48 which have narrow pore diameters. Similar results have been observed in other studies, being the SBA-15, the material with the higher pore size, the material with higher retention capacity (Vinu, Gokulakishnan, Mori & Ariga, 2008). Furthermore, each material tested has a different immobilization behaviour as a function of pH (Figure 2) but all of them present higher rate at pH 4.00. The silanol groups of mesoporous walls are negatively charged at this pH value (silanols show a pI around 2, see i.e. Cui, Zin, Cho & Ha, 2005)and the PPO, which has a pI value around 5.0 (Fan & Flurkey, 2004), is positively charged. Favourable electrostatic interactions thus, exist between the enzyme and the silica wall leading to adsorption and immobilization.

The other two pH values tested near from this value (pH 3.00 and 5.00) also present high immobilization rate. By contrast, the solutions far from pH 4 (pH 1.00 and 7.00) show almost no PPO immobilized - less than 100 mg of PPO per g of mesoporous material -. This behaviour can be explained because at these pHs both enzyme and material have the same charge (Fan y Furlkey 2014; Cui, Zin, Cho & Ha, 2005). At pH 1.00, both are charged positively; whereas at pH 7.00 both have a predominately negative charge.

In order to gain deeper insight about the immobilization process, all the kinetic curves were fitted by power law and Higuchi equations (Wise, 1985; Higuchi, 1961). These parameters are shown in

141 Table 2. Drug release data are frequently plotted as percent (or fractional) drug released versus
142 $t_{1/2}$ using the Higuchi model. Here, an attempt to do the same, but with loading amount instead
143 of release was done. A linear plot indicates a diffusional controlled drug loading (Higuchi, 1961).
144 The same curves were calculated fitting a power law equation and have a similar shape. Hence,
145 we can assume that the PPO immobilization into mesoporous materials is a diffusion controlled
146 mechanism. The coefficients of correlation of each model are considerably high. Table 2 shows
147 that the time needed to incorporate 50% of PPO depends directly on the pore size and volume of
148 the material. Materials with higher pore volume and pore size, such as SBA-15, need less than 1
149 min to incorporate the same quantity of enzyme as MCM-48 does in 2 hours.
150 The reported results show that the tested materials retain significant amounts of PPO. The good
151 response observed, together with the idea to develop a new and useful strategy for the food
152 industry encouraged us to further study the ability of SBA-15, the most active material, to
153 immobilize PPO directly from an apple extract. Apples (*Malus domestica*) were selected as they
154 are one of the most important sources of polyphenols (phenolic compounds) in the human diet
155 (Hertog, Hollman & Katan, 1992; Kammerer, D.R., Kammerer, J., Valet, R., & Carle, R., 2014) and a
156 classic example of fruit susceptible to enzymatic browning, which is a major problem for the fruit
157 processing industry (Coseteng & Lee, 1987; Rico, D., Martín-Diana, A.B., Barat, J.M., & Barry-Ryan,
158 C. 2007). Several studies have shown that enzymatic browning in apple pulp is associated with its
159 polyphenol content and/or polyphenol oxidase activity (Murata, Noda & Homma, 1995; Walker,
160 1964; Holdenbaum, D.F., Kon, T., Kudo, T., & Guerra, M.P., 2010).
161 As expected, in only 15 minutes the enzyme activity decreased to 51% of its original value,
162 however further time of contact does not increases significantly the inhibition for the
163 concentrations and conditions of the assay.
164

## 4. CONCLUSIONS

In conclusion, results suggest that silica based mesoporous materials offer a suitable approach for the development of new procedures of inhibition of the PPO in fruits and vegetables, in particular in apples. The enzyme immobilization is a diffusion controlled process in which the two main factors are pH and pore size. However, pore volume can be also relevant in particular with respect to the loading capacity. The highest immobilization rate was observed at a pH value of 4.00 probably because the electrostatic interactions are favourable between the enzyme and the silanol groups of the mesoporous walls. Wide pore size and volume materials such as SBA-15 offer the fastest and higher loading capacity with a loading of a 50% in only 15 minutes. These results suggest that SBA-15 can be an interesting material for the inactivation of PPO in juices and fresh cut fruits.

## NOTES AND REFERENCES


Anunziata, O.A., Beltramore, A.R., Martinez, M.L., & Bellon, L.L. (2007). Synthesis and characterization of SBA-2, SBA-15, and SBA-1 nanostructured catalytic materials. *Journal of Colloid Interface Science, 1:315(1)*, 184-190

Arroyo, M. (1998). Inmovilización de enzimas. Fundamentos, métodos y aplicaciones. *ArsPharmaceutica*, *39(2)***,** 23-39

Bernardos, A., & Kourimska, L. (2013). Applications of mesoporous silica materials in food- a review. *Czech Journal of Food Science*, *31(2)*, 99-107

Bradford, M.M. (1976). A rapid and sensitive method for the quantitation of microgram quantities of protein utilizing the principle of protein-dye binding. *Analytical Biochemistry*, *72*, 248-254

187 Coseteng, M.Y., & Lee, C.Y., (1987). Changes in Apple Polyphenoloxidase and Polyphenol
188 Concentrations in relation to Degree of Browning. *Journal of Food Science*, *52(4)*, 985-989
189 Cui, X., Zin, W-C., Cho, W-J., & Ha, C-S., (2005). Nonioinc triblock coploymer synthesis of SBA-15
190 above the isoelectric point of silica (pH =2-5). *Materials Letters, 59(18)*, 2257-2261
191 Datta, S., Christena, L.R., & Rajaram, Y.R.S. (2013). Enzyme immobilization: an overview on
192 techniques and support materials. *Biotechnology*, *3(1)*, 1-9
193 Denoya, G.I., Ardanaz, M., Sancho, A.M., Benítez, C.E., González, C., & Guidi, S. (2012). Efecto de la
194 aplicación de tratamientos combinados de aditivos sobre la inhibición del pardeamiento enzimático
195 en manzanas cv. Granny Smith mínimamente procesadas. *Revista de Investigación Agropecuaria*,
196 *38(3)*, 263-267.
197 Fan, Y., & Flurkey, W.H. (2004). Purification and characterization of tyrosinase from gill tissue of
198 Portabella mushrooms. *Phytochemistry*, *65(6)*, 671-678
199 Fu, C., Liu, T., Li, L., Liu, H., Chen, D., & Tang, F. (2013). The absorption, distribution, excretion and
200 toxicity of mesoporous silica nanoparticles in mice following different exposure routes. *Biomater*,
201 *34(10)*, 2565–2575.
202 Gacche, R.N., Zore, G.B., & Ghole, V.S. (2003). Kinetics and Inhibition of Polyphenol Oxidase Mediated
203 Browning in Apple Juice by B-Cyclodextrin and L-Ascorbate-2-triphosphate. *Journal of Enzyme*
204 *Inhibition and Medicinal Chemistry*, *18(1)*, 1-5
205 Guerrero, C.A., *Doctoral dissertation. Universidad Nacional de Colombia, Sede Medellín.* 2009
206 Higuchi, T. (1961). Rate of release of medicaments for ointment bases containing drugs in
207 suspension. *Journal of Pharmaceutical Sciences*, *50(10)*, 874-875
208 Kammerer, D.R., Kammerer, J., Valet, R., & Carle, R., (2014). Recovery of polyphenols from the by-
209 products of plant food processing and application as valuable food ingredients. *Food Research*
210 *International, 65,* 2-12

211 Kupferschmidt, N., Csikasz, R.I., Ballell, L., Bengtsson, T., Garcia-Bennett, A.E. (2014). Large pore
212 mesoporous silica induced weight loss in obese mice. *Nanomedicine*, *9(9)*, 1353-1362
213 Kupferschmidt, N., Xia, X., Labrador, R.H, Atluri, R., Ballell, L., & Garcia-Bennett, A.E. (2013). In vivo
214 oral toxicological evaluation of mesoporous silica particles. *Nanomedicine, 8(1)*, 57-64
215 Lu, J., Liong, M., Li, Z., Zink, J.I., & Tamanoi, F. (2010). Biocompatibility, biodistribution, and drug-
216 delivery efficiency of mesoporous silica nanoparticles for cancer therapy in animals. *Small*, *6(16)*,
217 1794-1805
218 Hertog, M.G., Hollman, P.C. and Katan, M.B. (1992). Content of potentially anticarcinogenic
219 flavonoids of 28 vegetables and 9 fruits commonly consumed in the Netherlands. *Journal of*
220 *Agricultural and Food Chemistry*, *40(12)*, 2379-2383
221 Holdenbaum, D.F., Kon, T., Kudo, T., & Guerra, M.P., (2010). Enzymatic Browning, Polyphenol Oxidase
222 Activity, and Polyphenols in Four Apple Cultivars: Dynamics during Fruit Development. *Hortscience,*
223 *45(8),* 1150-1154
224 Mangrulkar, P.A., Yadav, R., Meshram, J.S., Labhsetwar, N.K., & Rayalu, S.S. (2012). Tyrosinase-
225 immobilized MCM-41 for the detection of phenol. *Water, Air & Soil Pollution*, 819-825
226 Marín-Zamora, M.E., Rojas-Melgarejo, F., García-Cánovas, F., & García-Ruiz, P.A. (2009). Production
227 of o-diphenols by immobilized mushroom tyrosinase. *Journal of Biotechnology*, *139(2)*, 163-168
228 Murata, M., Noda, I.,& Homma, S. (1995). Enzymatic Browning of apples in the market: relation
229 between browning, polyphenol content and polyphenol oxidase. *Nippon Shokuhin Kogyo Gakkai-Shi*,
230 *42(10)*, 820-826.
231 Olivas, G.I., Mattinson, D.S., & Barbosa-Cánovas, G.V. (2007). Alginate coatings for preservation of
232 minimally processed “Gala” apples. *Postharvest Biology and Technology. Technol.*, 2007, *45(1)*, 89-
233 96

234 Olivier, J.P., Conklin, W.B.v., & Szombathely, M.V., 1994. Determination of Pore Size Distribution
235 from Density Functional Theory: A Comparison of Nitrogen and Argon Results. *Studies in Surface*
236 *Science and Catalysis, 87,* 81-89
237 Perez-Gago, M.B., Serra, M., & Del Rio, M.A. (2006). Color change of fresh-cut apples coated with
238 whey protein conntratea-based edible coatings. *Postharvest Biology and Technology*, *39(1)*, 84-92
239 Rocha, A.M.C.N., & Morais, A.M. (2001). Influence of controlled atmosphere storage on
240 polyphenoloxidase activity in relation to colour changes of minimally processes "Janagored" apple.
241 *International Journal of Food Science and Technology*, *36(4)*, 425-432
242 Rico, D., Martín-Diana, A.B., Barat, J.M., & Barry-Ryan, C. (2007). Extending and measuring the quality
243 of fresh-cut fruit and vegetables: a review. *Trends in Food Science & Technology, 18(7),* 373-386
244 Sapers, G.M., & Miller, R.L. (1993). Control of Enzymatic Browning in Pre-peeled Potatoes by Surface
245 Digestion. *Journal of Food Science*, *58(5)*, 1076-1078
246 Toribio, J.L., & Lozano, J.E., (1986). Heat Induced Browning of Clarified Apple Juice at High
247 Temperatures. *Journal of Food Science,* 1986, *51(1)*, 172-175
248 Vinu, A., Gokulakrishnan, N., Mori, T., & Ariga, K., (2008). Inmobilization of biomolecules on
249 mesoporous structured materials. Ed: Ruiz-Hitzky, E., Ariga, K., & Lvov, Y., *Wiley-VCH. Bio-inorganic*
250 *Hybrid Nanomaterials, chapter 4,* 113-158
251 Walker, J.R.L. (1964). Studies on the enzymic browning of apples. II. Properties of apple polyphenol
252 oxidase. *Australian Journal of Biological Sciences*, *17(2)*, 360-371
253 Wang, S., Wu, D., Sun, Y., & Zhong, B. (2001). The synthesis of MCM-48 with high yields. *Materials*
254 *Research Bulletin*, *36(9)*, 1717
255 Whitaker, J.R., & Lee, JC.Y. (1995). Recent Advances in Chemistry of Enzymatic Browning An
256 Overview. *ACS Symposium Series,* 1995, 2-7.

257 Wise, M.E., (1985). Negative power functions of time in pharmacokinetics and their implications.
258 *Journal of Phamacokinetics and Biopharmaceutics, 13*, 309–346.
259 Zhao, D., Feng, J., Huo, Q., Melosh, N., Fredrickson, G.H., Chmelka, B.F., & Stucky, G.D. (1998).
260 Triblock copolymer syntheses of mesoporous silica with periodic 50 to 300 angstrom pores. *Science*,
261 *279(5350)*, 548-552
262 Zhou, C., & Garcia-Bennett, A.E. (2010). Release of folic acid in mesoporous NFM-1 silica. *Journal of*
263 *Nanoscience and Nanotechnology*, *10(11)*, 7398-7401
264
265

**TABLE 1.** Textural parameters of calcined mesoporous materials calculated from nitrogen adsorption data.

| Material | Particle size[a] µm | Surface Area[b] ($m^2$/g) | MESOPOROUS | | MICROPOROUS | | |
|---|---|---|---|---|---|---|---|
| | | | Pore Volume[c] ($cm^3$/g) | Pore size[d] (Å) | Pore Volume[e] ($cm^3$/g) | Surface Area[e] ($m^2$/g) | Pore size[a] (Å) |
| SBA-15 | 1.3-1.5 | 411.8 | 1.00 | 133.0 | 0.023 | 66.3 | 25.2 |
| SBA-3 | > 5 | 1238 | 0.94 | 29.2 | - | - | - |
| MCM-48 | < 0.2 | 311,5 | 0.36 | 33.4 | - | - | - |

[a] Determined from SEM. [b] Surface area based on the Brunauer-Emmett-Teller (BET) equation. [c] From nitrogen adsorption isotherm. The pore volume is obtained from the total amount adsorbed at 0.98 in relative pressure. [d] Pore size derived from Density Functional Theory (DFT) model assuming cylindrical pore geometry. [e] Microporous parameters calculated from t-plot.

266

267

**TABLE 2.** Parameters of power law and Higuchi equations for the loading curves of PPO loading into mesoporous materials at pH 4.00.

| | Power law: $\ln F = \ln k_p + n \ln t$ | | | Higuchi: $F = k_H t^{1/2}$ | | |
|---|---|---|---|---|---|---|
| | $k_p$ | $n$ | $R$ | $k_H$ | $R$ | $T_{50\%}$ (min) |
| **SBA-15** | 0.87 | 0.01 | 1.00 | 0.02 | 0.97 | 0.10 |
| **SBA-3** | 0.28 | 0.32 | 0.99 | 0.27 | 0.80 | 18.04 |
| **MCM-48** | 0.76 | 0.37 | 0.99 | 0.74 | 0.91 | 131.32 |

$k_p$: kinetic constant; $n$: loading exponent; $R$: coefficient of correlation; $T_{50\%}$: the time loaded 50% of PPO; $k_H$ kinetic constant for the Higuchi model; $k_p$ for the power law model; $F$ is the equivalent to the rate of release in case of being applied to release.

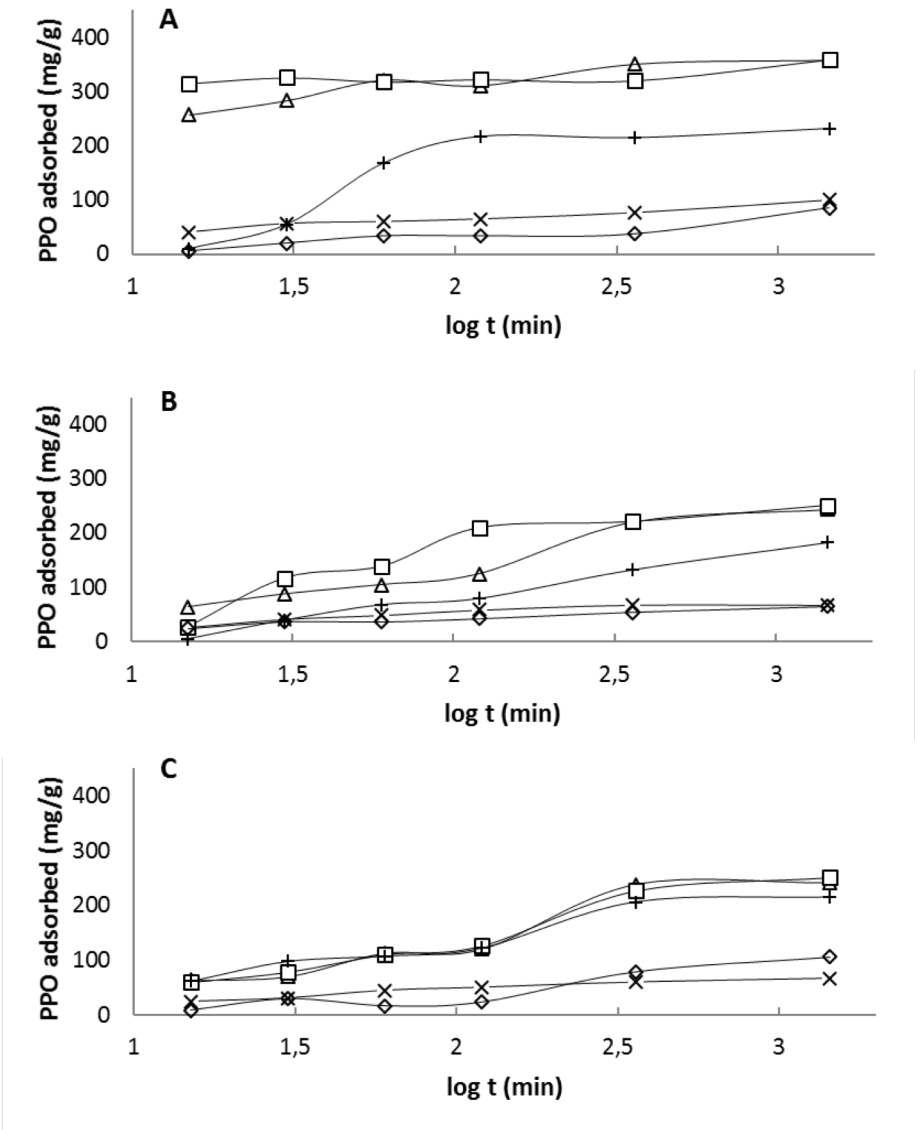


**FIGURE 1**. Immobilization kinetics of PPO (mg of enzyme / g mesoporous material) into the different materials at different pH values (x) pH1, (Δ) pH3, (□) pH4, (+) pH5, (◊) pH7.**A.** SBA-15 **B.** SBA-3 **C.** MCM-48.

271

272

273

274

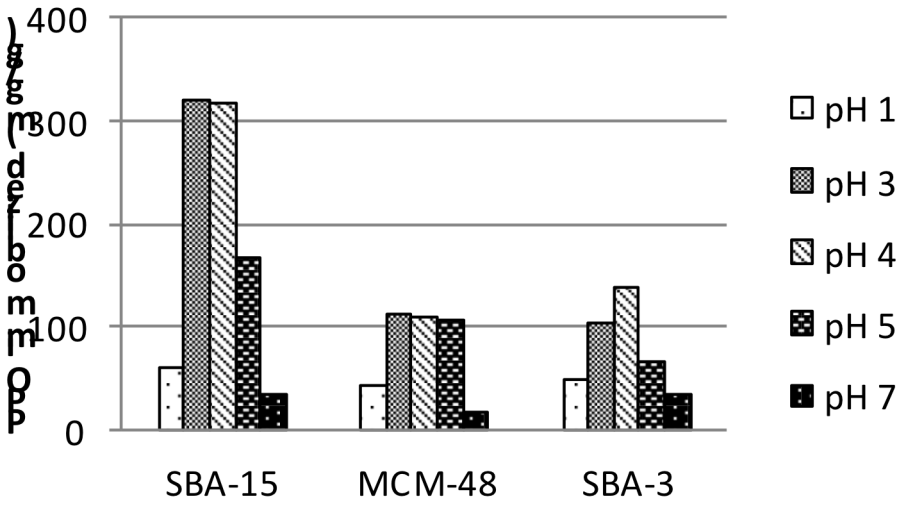


**FIGURE 2**. Amount of PPO adsorbed (mg of enzyme / g of mesoporous material) into the different materials at different pH values after 1 hour of immobilization assay.

275